Synthesis of TiO_2/SiO_2 Core/Shell Nanocable Arrays

Hongzhou Zhang,* Xuhui Luo, Jun Xu, Bin Xiang, and Dapeng Yu*

School of Physics, State Key Laboratory for Mesoscopic Physics, and Electron Microscopy Laboratory, Peking University, Beijing 100871, People's Republic of China

Received: January 16, 2004; In Final Form: July 8, 2004

Silica sheathed titania nanocable arrays were synthesized on Si substrates by using a vapor phase method. The morphology, microstructure, and chemical composition of the nanocables were characterized by using scanning electron microscopy, transmission electron microscopy, and spatial-resolution energy-dispersive X-ray spectroscopy, respectively. Raman spectroscopy combined with the other characterization methods elucidates that the nanocable core is of rutile titania. X-ray photoelectron spectroscopy indicates the existence of Ti−O−Si bonds as well as Ti−O−Ti and Si−O−Si bonds. A possible growth mechanism of the nanocables was also proposed on the basis of thermodynamic and kinetic considerations. The as-grown nanocable arrays may find applications as photocatalysts.

Introduction

Quasi-one-dimensional (1D) materials such as nanotubes, nanowires, nanobelts, and nanocables have attracted much attention.[1−4] Nanotubes, nanowires, and nanobelts grown from a variety of materials have been intensively investigated, and some cabled 1D structures have been studied as well. These nanostructures exhibit large aspect and surface-to-volume ratios, which can dramatically increase their effective surfaces and, thus, enhance their size-related properties exemplified by catalysis. As catalysts supporting many reactions, titania−silica materials have been widely used as photocatalysts, acid catalysts, and oxidation catalysts.[5] The catalytic function of titania−silica is mainly attributed to TiO_2, and SiO_2 has high thermal stability and excellent mechanical strength. Actually, TiO_2 itself has found applications in optoelectronic devices and industrial catalysis.[6] Pure titania nanoparticles, nanotubes, and nanowires have been synthesized by using diverse chemical routines, for example, sol−gel process, aqueous phase reaction, electrospining and calcinations, hydrothermal synthesis, and anodic oxidation.[7−11] On the other hand, amorphous silica nanowires have also been fabricated.[12] For the catalytic function of titania−silica mixtures and compounds, it is not a simple combination of the two species. The addition of silica can enhance the dispersion of titania and form Ti−O−Si bonds. In addition, the activity of TiO_2 can be improved substantially with the incorporation of silica.[13] The miniaturization of titania−silica materials, however, has hitherto been focused on the fabrication of nanoparticles.[14] To date, only a few examples of 1D titania−silica structures have been reported. Zhang et al. have documented coaxial TiO_2/SiO_2 nanotubes by using a sol−gel method with anodic alumina templates,[16] whereas, to our knowledge, the core/shell nanocables of titania−silica have not been synthesized. The other objective of this work is about the fabrication method; that is, almost all the existing routines for the fabrication of titania nanostructures are chemical methods;[7−13] is it possible to synthesis 1D titania−silica nanostructures by using a physical process? In this work, we demonstrated a simple but widely used vapor phase process to grow titania−silica nanocable arrays on silicon substrates. The structures and compositions of the as-grown nanocables were investigated, and a growth mechanism was proposed as well.

Experimental Section

The TiO_2/SiO_2 core/shell nanocable arrays were fabricated through a physical vapor process by evaporating Ti powders. An alumina crucible filled with pure Ti powders was placed at the middle of an alumina tube, which was heated by a tube furnace. A silicon slice was placed over the alumina crucible with the polished side facing the Ti powders. The pressure inside the tube was then pumped down to ~0.03 MPa, and during the growth process, the pressure was maintained by balancing the pumping rate and the flow of the carrier gas (Ar). Oxygen was introduced into the tube via the system leakage with an upper limit of flow of <5 sccm. The temperature at the source was first elevated to 850 °C, while the Ar gas was fed into the tube at a constant flow rate of 100 sccm. The growth lasted for 30 min. The alumina tube was then cooled to room temperature naturally. The silicon surface turned into a dark gray color, and the Ti source powders were fully calcined and turned into a dark gray color as well.

The morphology of the as-grown sample was first investigated by using a field-emission Strata DB235 workstation working in scanning electron microscopy (SEM) mode. A transmission electron microscope (Tecnai F30 operating at 300 kV) equipped with a Gatan image filter (GIF) system was used to further elucidate the structures and compositions of the sample. In addition to the conventional transmission electron microscopy (TEM) and high-resolution TEM (HRTEM) investigation, TEM observations and spatial-resolved energy-dispersive X-ray spectroscopy (EDS) analyses were also performed using scanning transmission electron microscopy (STEM). To prepare the TEM sample, the silicon surface was scratched by using sharp forceps. A little amount of ethanol was dropped onto a transmission electron microscope grid. We then dipped the tips of the forceps into the ethanol so that the scratched samples attached to the tips of the forceps could be transferred onto the transmission electron microscope grid. We also prepared a cross section

* Authors to whom correspondence should be addressed. E-mail: zhanghz@pku.org.cn (H.Z.); yudp@pku.edu.cn (D.Y.). Phone: +86-010-62759474. Fax: +86-010-62759474.

10.1021/jp049770d CCC: $27.50
Published on Web 08/25/2004

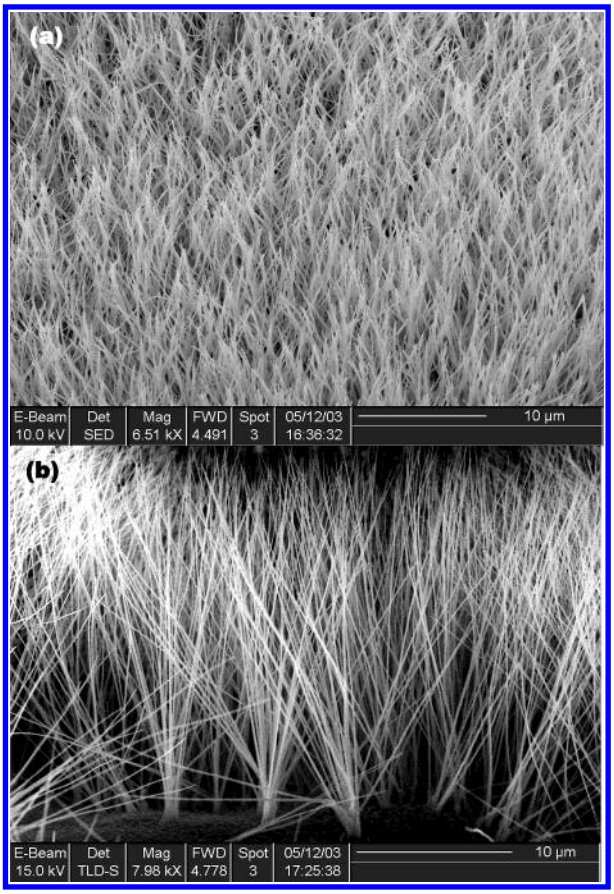

Figure 1. SEM images of the TiO_2/SiO_2 nanocable arrays: (a) top view; (b) titled view.

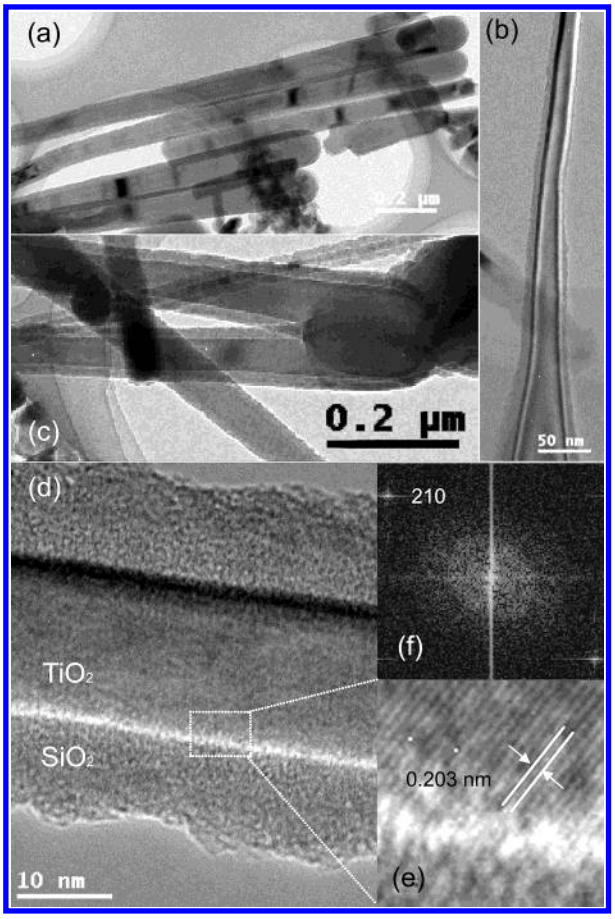

Figure 2. TEM images of the TiO_2/SiO_2 nanocables (a) showing a cabled structure, (b) revealing a tip of the nanocable, and (c) indicating two nanocables connecting at their roots. (d) High-resolution TEM image showing the crystal and amorphous nature of the core and the sheath, respectively; (e) a small part (indicated by the white dotted rectangle) is enlarged and shown displaying the lattice fringes in the core. (f) FFT image of the core region.

sample for STEM and EDS observation using conventional TEM sample preparation techniques. Raman scattering measurements were carried out to further analyze the structures of the products, and X-ray photoelectron spectroscopy (XPS) was used to depict the bonding information of the products.

Results and Discussion

The SEM images illustrated in Figure 1 reveal the general morphology of the TiO_2/SiO_2 core/shell nanocable arrays grown on Si substrates. Figure 1a, a top view of the sample surface, reveals a large amount of 1D nanocables covering the silicon surface uniformly. Such high and uniform coverage extends to several tens of micrometers in lateral dimensions on the surface of the Si substrate. Figure 1b is a tilted view of the sample surface indicating the 1D nature of the nanocables. The nanocables are over 20 μm long and several nanometers in diameter, demonstrating a large aspect ratio of the as-grown nanostructures ($\sim 10^3$). Figure 1b also shows that a few nanocables grew from the same spot on the substrate; that is, their roots combined, forming a bundle.

The microstructure of the sample was further analyzed by using TEM and HRTEM. A typical TEM image of the nanocables is shown in Figure 2a. The TiO_2/SiO_2 nanocables exhibit the shape of a straight rod. The core/shell structure can be observed clearly; the outer sheaths of the nanocables are brighter than the cores. The diameter of a typical nanocable increases from the tip ($\sim$20 nm) toward the end ($\sim$100 nm). The tip of one nanocable is magnified in Figure 2b, and the gradual shrinkage of its diameter is obvious. Figure 2c shows two nanocables connecting each other at their ends, as we have found in the SEM observation (Figure 1b). However, most of the nanocables observed in TEM investigation are separated, which may be due to the break of the nanocables during the preparation of the TEM sample. It can also explain why the measured lengths of the nanocables from TEM observation are usually shorter than those from SEM observation. The HRTEM image in Figure 2d can give further insight into the details of the structure. To clearly show the microstructure of core TiO_2, a small part of Figure 2d (indicated by the white dotted rectangle) is enlarged and shown in Figure 2e. The lattice fringes can then be distinguished clearly in the core, while the shell of 10 nm in thickness has an amorphous nature (see Figure 2d). The spacing between two fringes of the core is $\sim$0.203 nm, corresponding to the interplanar spacing of the (210) planes of the rutile TiO_2. The continuous fringes demonstrate that the core of the nanocables has a low defect density. The fast Fourier transform (FFT) of the core is shown in Figure 2f. The HRTEM observation together with its FFT supports that the core of the nanocables is a rutile TiO_2 structure.

To verify the chemical concentration profile of the nanocables and the substrate, we prepared a TEM cross section sample. STEM and EDS line scan analysis were performed across the cross section. Figure 3a is an STEM image of the sample cross section. The dashed line in Figure 3a indicates the location of the scan line of the spatial-resolution EDS, and the corresponding chemical concentration profile is shown in Figure 3b. The line scan enters from the core of a nanocable, crosses its root, and then enters the substrate. The increase of the counts at the

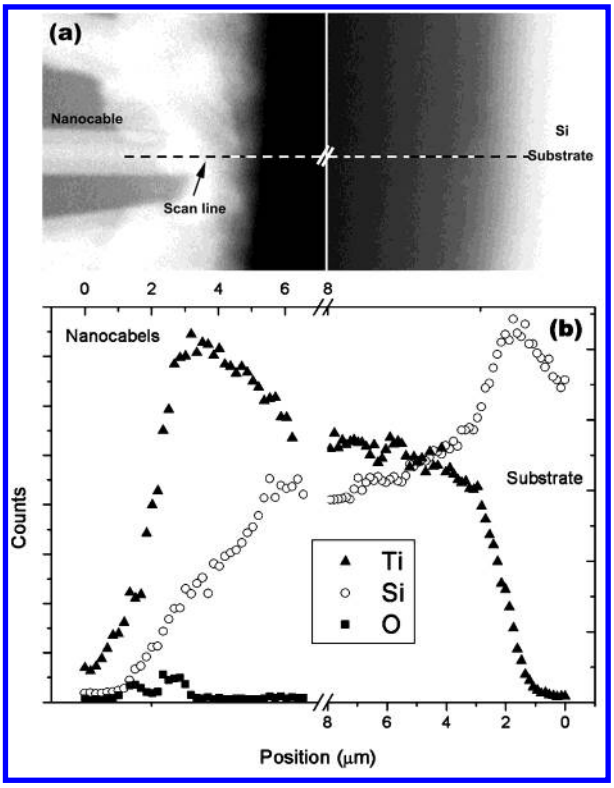

Figure 3. (a) STEM image of the sample's cross section with the dashed line indicating the EDS scan line. (b) Compositional profile of the EDS line scan suggesting the existence of a titanium silicide layer between the nanocables and the substrate.

root of the nanocable may be due to the increase of the sample thickness; therefore, we will only focus on the relative intensities of the three detected elements (Ti, Si, and O). It is found that the Ti species are dominant at the core of the nanocable. A Ti peak occurs at the root of the nanocable, suggesting the existence of abundant Ti at the root of the nanocable. As the scan leaves the nanocable and enters the substrate, the Ti signal can still be detected with almost an equal intensity to that of the Si signal. The Ti signal begins to decrease and eventually disappears when the scan penetrates the substrate ~10 μm deep and goes further. The results of the line scan analysis indicate that an accumulation of Ti occurs at the root of the nanocable as well as a layer of Ti−Si compound formed at the interface of the Si substrate and the nanocables.

Raman scattering has proven to be a versatile technique for characterizing nanostructured materials.[17] To further investigate the phase of these TiO_2/SiO_2 nanocables, we measured the Raman spectrum of the as-grown samples, and the result are shown in Figure 4. Two intensive peaks at 445 and 609 cm^{-1} are observed in the Raman spectra, which are attributed to the Raman scattering of the E_g mode and A_{1g} mode of rutile TiO_2.[18] The peak at 521 cm^{-1} arises from the Si substrate. Raman scattering demonstrated the existence of rutile TiO_2 in the samples. Combined with the HRTEM and EDS results, we can surely claim that the core of the nanocable is rutile TiO_2.

Ti is highly reactive with oxygen, while as a reducible oxide, it exhibits several phases with different stoichiometries. To further clarify the chemical situations of the elements, we measured the XPS of the samples. As is shown in Figure 5a, the binding energy of Ti $2p_{3/2}$ is 458.4 eV, which is consistent with the reported value of TiO_2 (458.7 eV with a standard deviation of 1.3 eV).[19] Also, the XPS profile of O 1s is shown in Figure 5b. The profile can be deconvoluted to three peaks, 530.7, 532.9, and 531.2 eV, which can be attributed to Ti−O−Ti, Si−O−Si, and Si−O−Ti bonds, respectively.[5] It is inferred that Si oxide in the sheath is combined onto core TiO_2 through a chemical bond of Ti−O−Si. In addition, the X-ray photoelectron spectroscopy indicates that there exists only the Ti^{4+} charged state in the sample rather than the other Ti oxidation states.

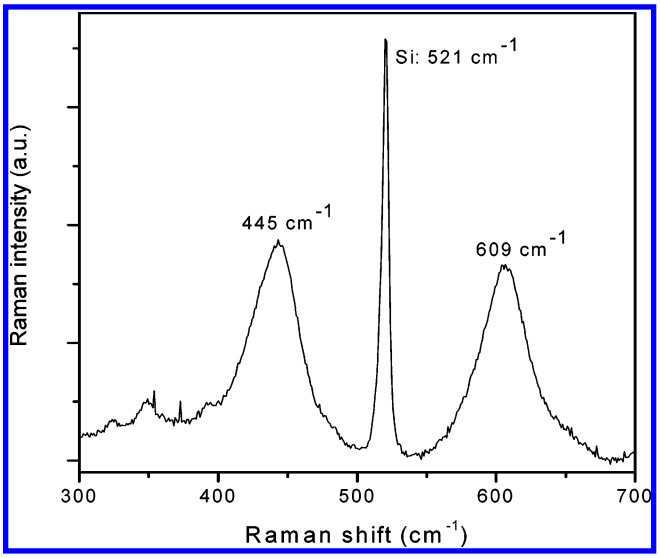

Figure 4. Raman spectrum of the as-grown samples demonstrating the structure of rutile TiO_2.

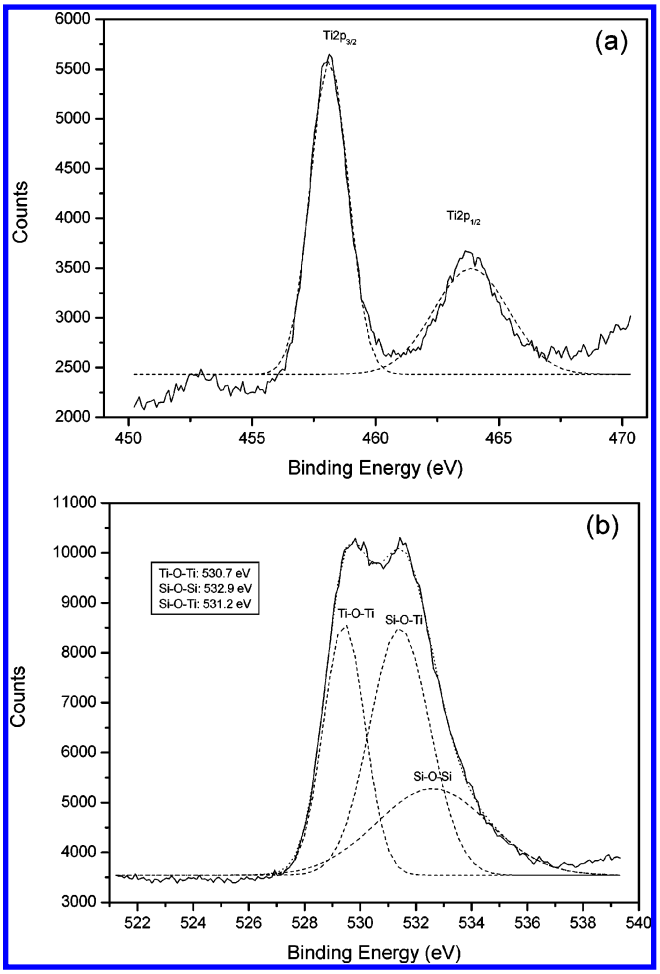

Figure 5. XPS spectra of the as-grown samples: (a) Ti 2p; (b) O 1s.

The growth mechanism of the TiO_2/SiO_2 nanocables can be understood by considering related thermodynamic and kinetic processes of the growth. For the thermodynamic consideration,

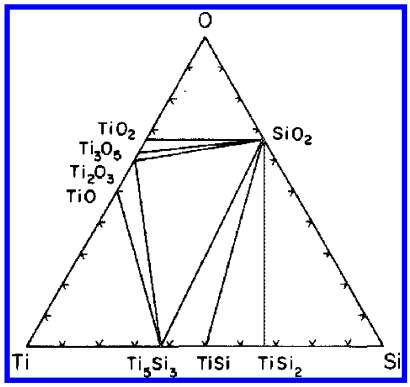

Figure 6. Ternary phase diagram of Ti−O−Si.[20]

we studied the Ti−O−Si ternary phase diagram, as shown in Figure 6.[20] At the early stage of the growth, a Ti species diffused onto the Si substrate and was adsorbed. In the context of the Ti−O−Si ternary phase diagram, no tie line exists between Ti and SiO_2, so native oxide found on Si is chemically unstable and will be broken down by reaction with Ti. Titanium silicide will form at this stage. Meanwhile, because the ambient growth is rich in Ti species, excess Ti may precipitate within the $TiSi_2$ during the formation of the $TiSi_2$ layer. On the other hand, however, the Ti source can be gradually oxidized by the ambient oxygen and the partial pressure of Ti decreases monotonically. The Ti precipitates within the $TiSi_2$ layer were first oxidized and then served as the nuclei of the cores of the nanocables. For the subsequent growth, the oxidation of $TiSi_2$ played an important role. It has been found that $TiSi_2$ dissociates and reacts with oxygen to form both a titanium compound and SiO_2 if silicon diffusion to the reacting interface becomes the rate-limiting step for the oxidation.[21] In our case, the surfaces of the TiO_2 nuclei provided the favorite reacting interface for the dissociation of $TiSi_2$. The formation of Ti oxide will result in an accumulation of excess Si. Calculations based on thermodynamic properties indicate that, at temperatures >700 °C when Si and $TiSi_2$ coexist, the only stable oxide is SiO_2.[20] Therefore, the SiO_2 layer will form and sheath the Ti oxide. At the roots of the nanocables, the growth sites of SiO_2 and TiO_2 may very well separate from each other. The growth of the SiO_2 depletes Si at the growth site of SiO_2 and makes excess Ti, while at the growth site of TiO_2, Si is the excess species by running out Ti. Therefore, this process established opposite concentration gradients for Si and Ti. They thus diffuse to their respective growth sites. We also point out that the thickness of the $TiSi_2$ layer exceeds 6 μm, which impedes the thermal diffusion of Si from the substrate to the surface of the $TiSi_2$ layer and the reacting interface. Otherwise, only SiO_2 is possible.[21]

Conclusions

In conclusion, silica sheathed titania nanocable arrays were synthesized on a Si substrate using a vapor phase method. SEM and TEM investigation demonstrated the nanocables have a large aspect ratio and high coverage on the substrate. EDS line scan analysis indicated a layer of titanium silicide with a thickness over 6 μm existing between the Si substrate and the nanocables. The roots of the nanocables also show a Ti abundant nature. The phase of the core titania is of a rutile structure determined by Raman spectroscopy measurement. X-ray photoelectron spectroscopy indicates the existence of Ti−O−Si bonds as well as Ti−O−Ti and Si−O−Si bonds. The growth of the nanocables is attributed to the separation of the growth sites of TiO_2 and SiO_2, which is a result of the thermodynamic and kinetic processes of the growth. However, further exploration of the inherent properties of these nanostructures, for example, photocatalysis behavior, is needed for realizing their potential applications.

Acknowledgment. This project was financially supported by the National Natural Science Foundation of China (NSFC, nos. 50025206 and 20151002,), the Scientific Research Foundation for the Returned Overseas Chinese Scholars (Grant No. EJ20030038), the State Education Ministry, the 31st Postdoc Research Foundation, and national 973 projects (no. 2002CB613505, MOST, P. R. China). D.Y. gratefully acknowledges the financial support from the Cheung Kong Scholar program.

References and Notes

(1) Iijima, S. *Nature* **1991**, *354*, 56−58.
(2) Morales, M.; Lieber, C. M. *Science* **1998**, *279*, 208−211.
(3) Pan, Z. W.; Dai, Z. R.; Wang, Z. L. *Science* **2001**, *291*, 1947−1949.
(4) Zhang, Y.; Suenaga, K.; Colliex, C.; Iijima, S. *Science* **1998**, *281*, 973−975.
(5) Gao, X.; Wachs, I. E. *Catal. Today* **1999**, *51*, 233−254.
(6) Justicia, I.; Ordejon, P.; Canto, G.; Mozos, J. L.; Fraxedas, J.; Battiston, A.; Gerbasi, R.; Figueras *Adv. Mater.* **2002**, *14*, 1399−1402.
(7) Lei, Y.; Zhang, L. D.; Meng, G. W.; Li, G. H.; Zhang, X. Y.; Liang, C. H.; Chen, W.; Wang, S. X. *Appl. Phys. Lett.* **2001**, *78*, 1125−1127.
(8) Kasuga, T.; Hiramatsu, M.; Hoson, A.; Sekino, T.; Niihara, K. *Adv. Mater.* **1999**, *11*, 1307−1311.
(9) Li, D.; Xia, Y. *Nano Lett.* **2003**, *3*, 555−560.
(10) Zhang, Y. X.; Li, G. H.; Jin, Y. X.; Zhang, Y.; Zhang, J.; Zhang, L. D. *Chem. Phys. Lett.* **2002**, *365*, 300−304.
(11) Gong, D.; Grimes, C. A.; Varghese, O. K.; Hu, W.; Singh, R. S.; Chen, Z.; Dickey, E. C. *J. Mater. Res.* **2001**, *16*, 3331−3334.
(12) Yu, D. P.; Hang, Q. L.; Ding, Y.; Zhang, H. Z.; Bai, Z. G.; Wang, J. J.; Zou, Y. H.; Qian, W.; Xiong, G. X.; Feng, S. Q. *Appl. Phys. Lett.* **1998**, *73*, 3076−3078.
(13) Liu, T. C.; Cheng, T. I. *Catal. Today* **1995**, *26*, 71−77.
(14) Lin, Y. L.; Wang, T. J.; Jin, Y. *Powder Technol.* **2002**, *123*, 194−198.
(15) Hua, Z. L.; Shi, J. L.; Zhang, L. X.; Ruan, M. L.; Yan, J. N. *Adv. Mater.* **2002**, *14*, 830−833.
(16) Zhang, M.; Bando, Y.; Wada, K. *J. Mater. Res.* **2001**, *16*, 1408−1412.
(17) Tan, P. H.; Brunner, K.; Bougeard, D.; Abstreiter, G. *Phys. Rev. B*, in press.
(18) Zhang, F.; Zheng, Z.; Liu, D.; Mao, Y.; Chen, Y.; Zhou, Z.; Yang, S.; Liu, X. *Nucl. Instrum. Methods Phys. Res., Sect. B* **1997**, *132*, 620−626.
(19) Diebold, U.; Madey, T. E. *Surf. Sci. Spectra* **1998**, *4*, 227−231.
(20) Beyers, R. *J. Appl. Phys.* **1984**, *56*, 147−152.
(21) Chen, J. R.; Houng, M. P.; Hsiung, S. K.; Liu, Y. C. *Appl. Phys. Lett.* **1980**, *37*, 824−826.